Published in final edited form as:
Anal Chem. 2007 September 15; 79(18): 7154–7160. doi:10.1021/ac071201p.

Kinetic Modulation of Pulsed Chrono-potentiometric Polymeric Membrane Ion Sensors by Polyelectrolyte Multilayers

Yida Xu[a], **Chao Xu**[a], **Alexey Shvarev**[b], **Thomas Becker**[c], **Roland De Marco**[c], and **Eric Bakker**[a]

Department of Chemistry, Purdue University, 560 Oval Drive, West Lafayette, Indiana 47907, Deparment of Chemistry, Oregon State University, Corvallis, OR 97331, and Department of Applied Chemistry, Curtin University of Technology, Perth, WA 6845, Australia

Abstract

Polymeric membrane ion selective electrodes are normally interrogated by zero current potentiometry, and their selectivity is understood to be primarily dependent on an extraction/ion-exchange equilibrium between the aqueous sample and polymeric membrane. If concentration gradients in the contacting diffusion layers are insubstantial, the membrane response is thought to be rather independent of kinetic processes such as surface blocking effects. In this work, the surface of calcium-selective polymeric ion-selective electrodes is coated with polyelectrolyte multilayers as evidenced by zeta potential measurements, atomic force microscopy and electrochemical impedance spectroscopy. Indeed, such multilayers have no effect on their potentiometric response if the membranes are formulated in a traditional manner, containing a lipophilic ion-exchanger and a calcium-selective ionophore. However, drastic changes in the potential response are observed if the membranes are operated in a recently introduced kinetic mode using pulsed chronopotentiometry. The results suggest that the assembled nanostructured multilayers drastically alter the kinetics of ion transport to the sensing membrane, making use of the effect that polyelectrolyte multilayers have different permeabilities toward ions with different valences. The results have implications to the design of chemically selective ion sensors since surface localized kinetic limitations can now be used as an additional dimension to tune the operational ion selectivity.

Polymer membrane ion-selective electrodes are widely established for the reliable assessment of ion activities in complex samples and are indispensable tools in clinical analysis. Their ion-selectivity is dictated by the thermodynamic ion-exchange selectivity of the polymer membrane. Recently, ion-selective membrane electrodes have started to be interrogated by pulsed chronopotentiometry. In this new technique, a discrete current pulse is imposed across an ion-selective membrane void of added ion-exchanger sites. The potential change associated with the resulting ion flux from the sample into the sensing phase can be monitored during or, at open circuit, immediately after the pulse before the membrane is regenerated under controlled potential conditions. At high sample concentrations the observed sensitivity (electrode slope) and selectivity normally agrees with that of the corresponding ion-selective electrodes interrogated at zero current.[1, 2] The imposed ion flux, however, depletes the analyte ions in the Nernst diffusion layer at a critical concentration, and very large (ca. 10-fold Nernstian) electrode slopes are observed in this concentration range.[3] The operational ion

Correspondence to: Eric Bakker.
[a]Purdue University
[b]Oregon State University
[c]Curtin University of Technology

selectivity of the sensor here is also governed by the kinetics of mass transport and ion transfer into the polymeric sensing phase, as also recently demonstrated with neutral surfactants.[4]

Ultra-thin films assembled from alternate adsorption of polycations and polyanions onto a charged substrate has attracted much attention in recent years due to their facile fabrication, high versatility and multi-functionality. The application of this technique has expanded into a number of areas, including biosensor surface modification,[5] gas permeation,[6] alcohol-water pervaporation,[7] nanofiltration[8] and patterning.[9] The adsorption properties are dependent on many factors, such as pH and ionic strength of supporting electrolyte,[10] charge density of polyelectrolytes used,[11] solvent quality[12] and temperature.[13] The characterization methods are very versatile, from ex-situ detection such as ellipsometry,[14] atomic force microscopy,[14] quartz crystal microbalance[15] and X-ray reflectivity,[16] to in-situ measurements such as streaming potential method,[17] attenuated total reflection,[18] neutron reflectivity[16] and scanning angle reflectometry.[19]

Recently, liquid-liquid interfaces coated with polyelectrolyte multilayers were studied utilizing conventional electrochemical methods such as AC voltammetry and cyclic voltammetry, and the multilayers exhibited a kinetic ion transfer hindrance.[20, 21] Through theoretical modeling, these authors demonstrated a dependence of the apparent transfer rate and charge distribution of monovalent ions on polyelectrolyte multilayers at such modified interfaces. Those multilayers were also more permeable to monovalent ions than multivalent ions, and the permeability of highly charged ions such as $Fe(CN)_6^{3-}$ and $Ru(NH_3)_6^{3+}$ will decrease quickly when polyelectrolyte multilayers are assembled.[22] The slower diffusion with increased number of multilayer is attributed to the reduction of active area of charge transfer, and the active area may be merely a few spots on the film surface that are preferable to the transport of ions.[22] Farhat and Schlenoff used linear sweep voltammetry to study the transport of redox-active ferrocyanide and ferricyanide through heavily charged polyelectrolyte multilayers and explained the transfer of ions in the film as hopping between fixed “reluctant” ion exchange sites in the polyelectrolyte layers coming from the charge balance of the outermost polycations or polyanions.[23] Due to Donnan-enhanced membrane inclusion, the diffusion of negative ions in the polyelectrolyte multilayers bearing a positively charged surface will be facilitated.[23] The separation of monovalent and divalent ions can be very effective when the number of adsorbed layers and the charge density of polyelectrolyte are increased, for example, the selectivity α for sodium/magnesium may reach 112.5 with 60 layers of poly(allylamine hydrochloride) and poly(styrenesulfonate).[24]

The blocking effect of polyelectrolyte multilayers has also been applied to glucose sensors. The response of this amperometric sensor designed by the group of Heller is diffusion controlled by assembling the polyelectrolyte layers as an outer membrane on the electrode that contains the enzyme.[5] Diffusion of glucose across the outer membrane was shown to become the rate-limiting step, reducing the influence of enzyme stability on sensor response. The polyelectrolyte coating was also shown to eliminate interferences from other sample species, resulting in a higher sensor selectivity.

In this work, polycation poly(ethyleneimine) (PEI) was alternately deposited with polyanions such as bovine serum albumin (BSA), poly(acrylic acid) (PAA) and poly(styrene sulfonate) (PSS) in a layer-by-layer fashion onto calcium-selective polymeric membrane electrodes. The multilayers are characterized by zeta potential measurements, atomic force microscopy (AFM) along with electrochemical impedance spectroscopy (EIS), and the resulting modified membranes are interrogated by zero current potentiometry and pulsed chronopotentiometry to explore the effect of polyelectrolyte layers on the selectivity of the sensors.

Experimental

Reagents

PEI (poly(ethyleneimine); 25,000 daltons, Aldrich), PSS (poly(sodium styrenesulfonate); 500,000 daltons, Polysciences), PAA (poly(acrylic acid); 450,000 daltons, Aldrich), PAH (poly(allylamine hydrochloride); 15,000 daltons, Aldrich), BSA (bovine serum albumin; 66,000 daltons, Sigma). 3-(trimethoxysilyl)propylmethacrylate was purchased from Sigma-Aldrich without further purification. High molecular weight poly(vinyl chloride) (PVC), 2-nitrophenyloctyl ether (o-NPOE), tetradodecylammonium tetrakis-(4-chlorophenyl)borate (ETH 500), potassium tetrakis(4-chlorophenyl) borate (KTpClPB) tetrahydrofuran (THF), and all salts were purchased from Fluka Chemical Corp. (Milwaukee, WI). Ultrapure silica gel was purchased from Silicycle chemical division. Calcium ionophore N, N-Dicyclohexyl-N′-phenyl-N′-3-(2-propenoyl)-oxyphenyl-3-oxapentanediamide (AU-1) was synthesized before in our group.[25] Aqueous solutions were prepared by dissolving the appropriate salts in Nanopure-deionized water (18.2 MΩ cm).

Electrodes

The ion-selective membranes for chrono-potentiometry experiments contained 20 mmol/kg AU-1, 10% wt. lipophilic salt ETH 500, and PVC and o-NPOE have a mass ratio of 1:2. Zero-current potentiometry membranes contained 5 mmol/kg KTpClPB instead of ETH 500 with all other components remaining the same. The membranes were cut with a cork borer (6-mm diameter) from the parent membrane and incorporated into Philips electrode bodies (IS-561, Glasbläserei Möller, Zürich, Switzerland). For chronopotentiometry experiments, the inner solution consisted of 0.1 M NaCl (10 mM Tris-HCl buffer, pH 7.4) and was contacted with an internal Ag/AgCl electrode. For potentiometry measurements, the inner filling solution contained 10 mM calcium chloride. The electrodes were conditioned overnight before experiments in a solution identical to the inner filling solution. A double-junction Ag/AgCl electrode with a 1 M LiOAc bridge electrolyte was used as an external reference electrode.

Experimental Setup

Chronopotentiometry measurements were conducted in a three-electrode cell system where the Philips body electrode acted as a working electrode and the external reference electrode and counter electrode (platinum wire) were immersed into the sample. The pulsed galvanostatic/potentiostatic technique was utilized in galvanostatic control of the ion-selective membrane, which was described in detail elsewhere.[26] The chronopotentiometry experiments were performed with an AFCBP1 bipotentiostat (Pine Inst., Grove City, PA) controlled by a PCI-MIO-16E4 interface board and LabVIEW Software (National Instruments, Austin, TX) on a Macintosh computer. Prior to the experiment, the operation of the first electrode output of the bipotentiostat (K1) was switched to current control with potentiostatic control of output of second working electrode (K2). To apply the current pulse, the working electrode was connected to the K1 output via an analog switch controlled by external software. When the baseline potential between current pulses was applied, the working electrode was connected to the K2 output. During the experiments, each applied constant current pulse (of 1-s duration) was followed by another constant zero current pulse (of 0.5-s duration), then a constant potential pulse (of 15-s duration) was added. Sampled potentials, which represent the sensor response, were obtained as the average value during the last 100 ms (for current pulse) or 50 ms (for zero current pulse) of each current pulse. Zero-current potentials were measured with a 16-channel EMF monitor (EMF16, Lawson Labs, Phoenixville Pike, PA).

Polyelectrolyte multilayer assembly

The polyelectrolyte layers were deposited onto the electrode membrane surface by immersing the electrode in the designated polyelectrolyte buffer solution for a specific time as described in the following text. Subsequently, the electrode surface was rinsed with the same buffer before electrochemical measurement. All solutions were buffered to pH 7.4 with 10 mM Tris-HCl buffer in 0.1 M sodium chloride background.

Electrochemical impedance spectroscopy measurement

All EIS studies were undertaken using a Princeton Applied Research Parstat 2273 instrument. Experimental control and data acquisition was performed using a personal computer running the PowerSINE software. EIS spectra were collected at the open circuit potential using A.C. amplitude of ±10 mV rms and a frequency range of 100 kHz–100 mHz.

Preparation of silica gel microspheres overcoated with polyelectrolyte layers

Silanized silica gel particles of 40–63 μm in diameter were used to prepare the substrate for growth of polyelectrolyte layers. Briefly, blank Silica gel particles were first washed thoroughly with toluene to remove impurities, dried, and subsequently mixed with 3-(trimethoxysilyl)propylmethacrylate (10% v/v in toluene) in a flat-bottom reactor. The reaction mixture was heated to 60~70°C for 3 hours with water reflux. Excessive reagents and solvent were later removed and the particles were dried at room temperature. Silanized silica gel particles (375 mg) were doped with 5 mL THF solution containing a total mass of 75 mg doping ingredients mimicking the composition of the PVC based membrane used in chrono-potentiometry experiments, i.e. 0.8 mg AU-1, 7.5 mg ETH 500, 22.3 mg PVC and 44.5 mg NPOE. The slurry was mixed well, and then covered with aluminum foil for 48 hours. The sensing ingredients were introduced into the porous silica templates upon evaporation of the solvent. The microspheres loaded with membrane components were used as the substrate for the growth of polyelectrolyte layers. Loaded silica gel particles were transferred to a 2-mL centrifuge vial, where 1 mL of polyelectrolyte solution was added and let settle. After 30 min the mixture was centrifuged for 3 min and the solution was discarded. A 0.1 M NaCl solution (1 mL) in 10 mM Tris-HCl buffer was added to the centrifuge vial with the precipitated particles for rinsing, followed with another 3 min of centrifugation. The buffer solution was then purged and the precipitated particles were kept in the original vial until the zeta potential measurement.

Zeta potential measurements

Solutions of 10 mg of dry colloidal particles in 20 mL of 1 mM Tris-HCl buffer (pH 7.4) were prepared for the zeta potential measurements. The ζ potential was measured using zeta-meter 3.0 (zeta-meter company, Inc.) based on 20 measurements. Carb ZeissDR microscope was used to observe the particle moving under the electric field of 50–100 V in an electrophoresis cell.

AFM measurements

The topography of the membranes and the polyelectrolyte multilayers were characterized using a small-range multipurpose scanner of a PicoPlus AFM system (Molecular Imaging/Agilent Technologies, Tempe, Arizona, USA). All AFM measurements were performed in Tapping Mode in solution with silicon nitride probes DNP (Veeco, USA) with a spring constant of k = 0.32 N/m and a resonant frequency of ν_{res} = 13.14 kHz (in solution). The images were scanned with a scan rate of 2 Hz at room temperature. Phase imaging was performed in order to get more detailed information about the fine structure of the polyelectrolyte layers. The membranes for the AFM surface characterization were obtained via dip-coating a freshly cleaved mica disc (Holgate Scientific Pty Ltd, NSW, Australia) into a solution of the membrane components dissolved in THF. The blank PVC membrane was imaged in-situ in 0.01 M Tris and the

polyelectrolyte layers were imaged in solutions of polyethyleneimine and albumin in Tris-buffer, respectively. After injecting the solution into the fluid cell of the AFM system, the system was equilibrated for about 20 minutes before starting to scan the samples. The AFM data were collected at room temperature with a scan rate of 2 Hz.

Results and Discussion

Polycations and polyanions were assembled onto calcium-selective membrane surfaces as described in the experimental section. To demonstrate the successful alternate adsorption of polyions, zeta potential measurements were performed on silanized silica gel particles doped with the same sensing material as used in the chronopotentiometric calcium-selective membrane experiments described below. The silanization of silica gel particles will effectively neutralize their surface charge, in contast to to regular silica particles that always carry negative charges. The silanized particles doped only with polymeric membrane material were found to exhibit a negative surface charge, which suggests the possibility of subsequent polycation adsorption. The ζ potential was found to alternate between positive and negative values with corresponding polycation (PEI) and polyanion (PAA) assembly, as shown in Figure 1. The amplitude of potential was found to vary for each type of polyion, resulting from the different charge densities of the polyeletrolytes and the heterogeneity of the silica particle size, which is in the range of 40–63 μm. The morphology of the multilayers adsorbed on the membrane surface was characterized by tapping mode AFM, which is depicted in Figure 2 as images of consecutive alternating polyelectrolyte multilayers adsorbed on a calcium selective membrane surface. The membrane coated with multilayers shows a significantly different morphology from a bare membrane surface. The PEI coating shows rod-like nanostructures while the albumin surface exhibits larger, globular configurations.

Some polyions, such as protamine and heparin, have a strong tendency to extract into appropriately formulated polymeric membranes and can result in a potential signal change in both zero-current potentiometry[27] and chrono-potentiometry[28], which has been used successfully for chemical sensing purposes. In this work, of course, extraction of any of the polyionic species used to build the multilayer assembly was not desired since we aimed at studying the influence of kinetic surface blocking on the sensor response. Figure 3 shows the zero current potentiometric responses of a calcium-selective membrane with subsequent coatings of PEI and BSA in a background of 0.1 M sodium chloride at pH 7.4. For up to 3 layers, the highest potential difference is found as about 3 mV upon coating. This important result has two implications. One, the calcium-selective membrane has no remarkable tendency to extract any of the polyions used here. Two, if any surface blocking takes place, zero current potentiometry is remarkably indifferent to it. This confirms current knowledge of the field, where the potential response is explained by localized extraction equilibria. If surface coatings are incapable of influencing this equilibrium state, it is of no consequence to the sensor response.

The influence of polyelectrolyte coatings was further explored with pulsed chronopotentiometric sensors. These employ essentially the same type of membranes, but avoiding ion-exchanger properties. A discrete current pulse results in an ion flux of fixed magnitude in direction of the membrane, and the observed potential at the same membrane is a function of the localized ion distribution resulting from the pulsed galvanostatic perturbation. The experiments were here performed with calcium-selective membranes in contact with sample solutions containing varying concentrations of calcium chloride in a constant sodium chloride background. Consequently, three concentration regions are important. At very low calcium concentrations, only the flux of sodium ions is relevant. Since only one type of ion is extracted, and the flux is instrumentally controlled, polyelectrolyte coatings are expected to have no effect on the observed potentials in this region. At intermediate calcium concentrations,

calcium and sodium fluxes compete with each other. If surface blocking of calcium takes place, sodium will better compete kinetically, and large effects of the polyelectrolyte coatings on the potential response are expected. At very high calcium concentrations, calcium should now be the dominant extracting ion and polyelectrolyte layers should again play a diminishing role on the potential response of the membrane.

The experimental pulstrode response of 3-layer successive alternate adsorption of PEI and BSA are shown in Figure 4. The signals were sampled first at the end of a 1-s cathodic current pulse with current density of 0.5 $\mu A/cm^2$, and subsequently another 0.5-s zero current pulse was applied and the response recorded. At last, a 15-s 0 V potential pulse was imposed to strip the ions out of the membrane. Without polyelectrolyte coating, the response of the membrane to continuous addition of calcium chloride exhibited a significant apparent super-Nernstian jump at around 10 μM. This confirmed a high discrimination of the background sodium ions and established the region of competitive extraction of sodium and calcium ions where polyelectrolyte layers are expected to influence the chronopotentiometric response, see above.

When the calcium-selective membrane was continuously immersed for 30 min in 5 g L^{-1} PEI solution (in the same Tris buffer), the potentials sampled at the end of each current pulse and zero current pulse were found to gradually decrease with time, and to stabilize to 15 mV and 3 mV relative to their initial values, respectively (data not shown). Since changes in the zero current potential were so small, the potential drop may be explained as an *iR* drop across the growing polyelectrolyte film. After the sensing membrane was taken out of the PEI solution and washed with Tris buffer, the calcium calibration process was repeated under the same conditions. The apparent super-Nernstian step in the calcium calibration curve was found to shift to higher calcium concentrations by about 1 order of magnitude, while the baseline potential for 0.1 M sodium chloride (without calcium) only decreased by about 6 mV. The smaller change of the response of sodium compared to the potential at the end of the dipping process may come from the washing step, since weakly adsorbed polyelectrolyte can be rinsed out.[29] As explained above, the shift in the apparent super-Nernstian step can be explained as an increased hindrance to the mass transport of calcium ions caused by the polycation coating. The location of this step is determined by the mass transfer hindrance of primary ions and correlates well with the known effect that polycations will decrease the permeation rate more effectively for divalent compared to monovalent ions.[24] The same procedure of immersion and calibration were repeated twice with BSA and PEI, and the effect of calcium blocking continued to be observed, as shown in Figure 4. The increased blocking of calcium ion diffusion was always observed, no matter whether the outermost layer carried a positive or negative charge. The thermodynamic selectivity of the sensor membrane was not significantly altered, since the baseline potential for 0.1 M sodium chloride totally only changed about 19 mV for the current pulse and 11 mV during the zero current pulse. Also, at the highest concentration range of calcium in the sample, the potential was rather independent of the polyelectrolyte assembly, especially for the zero current pulse. This shows that the calcium extraction thermodynamics is indeed not significantly influenced by the polyelectrolyte multilayer coating. The addition of just three polyion layers gives rise to a two-orders of magnitude shift of the calcium super-Nernstian step, suggesting that this type of diffusion barrier is remarkably effective for kinetically discriminating against calcium transport, thereby decreasing the kinetic selectivity of calcium over sodium in this concentration range.

Figure 5 illustrates the time trace for the potentials recorded at the end of each 1-s current pulse for the response of successive coverage of PEI, BSA and PEI on the calcium-selective membrane surface when the sample electrolyte contained 0.1 M sodium chloride and 1 mM calcium chloride (Tris pH 7.4). The stepwise potential drop also illustrates the diffusion hindrance of calcium upon adsorption of polyelectrolyte layers. The potential is very stable

even when the membrane is coated, which is indicative of the effective regeneration of the calcium-selective membrane after each 3-step pulse cycle.

Electrochemical impedance spectroscopy is a powerful electrode kinetic technique that can be used to probe the electric and dielectric behavior of electrode materials, and it has been employed extensively in mechanistic and optimization studies of electrochemical sensors including polymeric ion sensors.[30] Accordingly, to corroborate the result from the pulsed chronopotentiometric experiments, a parallel EIS measurement was performed under the same experimental conditions. In the complex-plane plot of Figure 6, the so-called Warburg diffusion impedance, as expressed by a phase shift of 45° at low frequencies for the blank sensing membrane, is increased when polyelectrolyte multilayers are coated. This gives rise to the apparent trend toward distorted low frequency semicircles which may comprise a convolution of the Warburg diffusion impedance and the ion transfer resistance.[31] In the corresponding Bode phase plot (Figure 6B), the phase shift of the second time constant in the low and medium frequency region is increased upon deposition of polycations and polyanions, which is indicative of polyelectrolyte coating on the membrane surface. A clearly defined polyelectrolyte film EIS time constant was not evident, possibly due to the nanoporous structure of the films.

The kinetic selectivity tuning function of polyelectrolyte coatings on calcium-selective membranes was further explored by choosing a divalent ion in the background electrolyte. The calcium calibration was performed in either a background of 0.1 M sodium chloride in 10 mM Tris or 25 mM magnesium sulfate in the same buffer, respectively, before and after continuous coating of PEI, BSA and PEI. The concentration of magnesium sulfate was chosen here to keep the same ionic strength, which otherwise may alter the structural properties of the adsorbed polyelectrolytes.[10] As shown in Figure 7, the potential baseline decreased dramatically, by about 100 mV, with the magnesium sulfate background when the three polyelectrolyte layers were present. On the other hand, a sodium chloride background resulted in a baseline shift of just 13 mV (current pulse) and 7 mV (zero current pulse), see inset of Figure 7. The much lower potential readings for the magnesium background confirm that this ion is thermodynamically strongly discriminated against. Surprisingly, the presence of polyelectrolyte multilayer suggests an even stronger discrimination. It should be very unlikely that partially extracted polyions actually destabilize magnesium ions in the membrane. A more convincing explanation is that the multilayer membrane blocks access of unspecified interfering cations, such as an impurity or the buffer species.[32] Indeed, the reported selectivity coefficient for ion-selective membranes based on this ionophore in PVC–NPOE is $K_{Ca,Mg}^{pot} = -8.7$,[25] which is only consistent with the potential change found for the membrane covered with the polyelectrolyte membrane. Since the baseline potential is changed so much upon adding the multilayer structure, quantitative discussion of the shift in the calcium super-Nernstian response region is difficult. While some shift is apparent relative to a sample with sodium electrolyte, it is rather insignificant. This implies that polyelectrolyte layers act primarily as diffusion membranes, in accordance with recent biosensor work.[5] The background cation, here sodium or magnesium, is in large excess compared to calcium in the concentration range of interest. Any reduction in the mass transport of calcium across the membrane will be compensated for by increased mass transport of the abundant background electrolyte. Hence, the super-Nernstian response region is not a strong function of the nature of this background electrolyte.

To investigate the effect of the charge density of polyelectrolyte multilayers on the kinetic selectivity adjustment of pulstrodes, two more polyanions, PSS and PAA, were examined with the same polycation, PEI. The experimental conditions were the same as for Figure 4, except that the concentration of PAA was reduced to 0.75 g L^{-1} to allow for buffering at the same pH. For the same reason a longer deposition time of 45 min was required, as evidenced by the

time the potential required to stabilize during the deposition process. Figure 8 presents the pulsed chronopotentiometric response to mixtures of calcium and sodium ions with two double layers formed by the alternate adsorption of PEI and PAA. An outermost PEI layer shifted the calcium response jump to higher concentrations, as in Figure 5, but when PAA was present as the last layer, a shift in the reverse direction, to lower concentrations than for the blank experiment, was observed. When the second double layer was adsorbed with PAA as the outmost layer, this shift was even more obvious, see Figure 8. We then explored one more polyanion, PSS, again with PEI as polycation. The super-Nernstian step in the calcium calibration curve shifted back after the adsorption of PSS, almost overlapping with the calibration curve of the bare calcium membrane. Compared to BSA, the most significant difference among these polyanions is likely their charge density, which is much smaller for BSA than for PSS and PAA. The high negative charge density may attract more calcium ions to the membrane surface compared to sodium ions, since electrostatic interactions will be stronger for divalent than monovalent ions. This process may partly compensate for the membrane diffusion barrier characteristics, resulting in a shift of the response to calcium ions to a lower concentration range. If the surface charge density is not sufficiently high, as with BSA, the diffusion barrier induced by polyelectrolyte coating will play the most important role and subsequent layers will mainly act as diffusion barriers as well.

Conclusions

Polyelectrolyte multilayers were alternately deposited on the surface of calcium-selective membranes. As expected, these multilayers appear to have a negligible effect on the extraction thermodynamics of the calcium-selective membrane. This was mainly evidenced by a complete lack of influence of polyelectrolyte multilayers on the traditional potentiometric response of such calcium-selective membranes. In pulsed chronopotentiometric measurements, three concentration dependent response regions can be distinguished. The lower and upper ranges are governed by single ion extraction processes and are not strongly affected by the presence of polyelectrolyte films. The so-called super-Nernstian response region, where the background electrolyte cations kinetically compete with the calcium ions that are partially depleted at the membrane surface, shows orders of magnitude shifts to higher calcium concentrations. An increased charge density of the outermost polyanion layers is found to move the super-Nernstian response region back to lower calcium concentrations, presumably because of ion accumulation effects at the polyelectrolyte surface. This particular study was mainly of mechanistic nature, and aimed at exploring the conditions under which the kinetics of ion transfer may show important influences in electrochemical ion sensors based on polymeric membrane electrodes. Evidently, traditional potentiometric sensors are rather robust with regards to such effects. Pulsed chronopotentiometric sensors are more prone to kinetic effects if measured in the concentration region where concentration polarization in the diffusion layer at the sample side of the membrane is prevalent. This may be understood as a potential limitation of the technique in view of measurements in biological or environmental samples, where surfaces may change with time. It may also have useful implications and result in measurement principles that rely on polymeric ion sensing materials that are exquisitely sensitive to compositional changes at the liquid–polymer interface. Indeed, affinity biosensing principles on the basis of such ion channel mimetic effects are currently under investigation in our laboratory.

Acknowledgments

The authors gratefully acknowledge financial support from the National Institutes of Health (GM07178) and the Australian Research Council (LX0454397 and DP0665400) for this research. We also thank Mr. Graeme Clarke for technical assistance with the AFM characterization of adsorbed polyelectrolytes.

References

1. Shvarev A, Bakker E. Anal Chem 2003;75:4541–4550. [PubMed: 14632062]
2. Makarychev-Mikhailov S, Shvarev A, Bakker E. J Am Chem Soc 2004;126:10548–10549. [PubMed: 15327306]
3. Makarychev-Mikhailov S, Shvarev A, Bakker E. Anal Chem 2006;78:2744–2751. [PubMed: 16615788]
4. Xu Y, De Marco R, Shvarev A, Bakker E. Chem Commun 2005:3074–3076.
5. Chen T, Friedman KA, Lei I, Heller A. Anal Chem 2000;72:3757–3763. [PubMed: 10959960]
6. Stroeve P, Vasquez V, Coelho MAN, Rabolt JF. Thin Solid Films 1996;284–285:708–712.
7. Krasemann L, Tieke B. Chem Eng Technol 2000;23:211–213.
8. Bruening ML, Stanton BW, Harris JJ. Polym Prepr 2004;45:43.
9. Shi F, Wang Z, Zhao N, Zhang X. Langmuir 2005;21:1599–1602. [PubMed: 15697313]
10. Steitz R, Jaeger W, von Klitzing R. Langmuir 2001;17:4471–4474.
11. Glinel K, Moussa A, Jonas AM, Laschewsky A. Langmuir 2002;18:1408–1412.
12. Poptoshev E, Schoeler B, Caruso F. Langmuir 2004;20:829–834. [PubMed: 15773111]
13. Buescher K, Graf K, Ahrens H, Helm CA. Langmuir 2002;18:3585–3591.
14. Mendelsohn JD, Barrett CJ, Chan VV, Pal AJ, Mayes AM, Rubner MF. Langmuir 2000;16:5017–5023.
15. Lvov Y, Ariga K, Onda M, Ichinose I, Kunitake T. Colloids Surf, A 1999;146:337–346.
16. Steitz R, Leiner V, Siebrecht R, v Klitzing R. Colloids Surf, A 2000;163:63–70.
17. Adamczyk Z, Zembala M, Warszynski P, Jachimska B. Langmuir 2004;20:10517–10525. [PubMed: 15544380]
18. Muller M, Heinen S, Oertel U, Lunkwitz K. Macromol Symp 2001;164:197–210.
19. Ladam G, Schaad P, Voegel JC, Schaaf P, Decher G, Cuisinier F. Langmuir 2000;16:1249–1255.
20. Malkia A, Liljeroth P, Kontturi AK, Kontturi K. J Phys Chem B 2001;105:10884–10892.
21. Slevin CJ, Malkia A, Liljeroth P, Toiminen M, Kontturi K. Langmuir 2003;19:1287–1294.
22. Barreira SVP, Garcia-Morales V, Pereira CM, Manzanares JA, Silva F. J Phys Chem B 2004;108:17973–17982.
23. Farhat TR, Schlenoff JB. J Am Chem Soc 2003;125:4627–4636. [PubMed: 12683835]
24. Krasemann L, Tieke B. Langmuir 2000;16:287–290.
25. Qin Y, Peper S, Radu A, Ceresa A, Bakker E. Anal Chem 2003;75:3038–3045. [PubMed: 12964748]
26. Shvarev A, Bakker E. Talanta 2004;63:195–200. [PubMed: 18969419]
27. Ramamurthy N, Baliga N, Wahr JA, Schaller U, Yang VC, Meyerhoff ME. Clin Chem 1998;44:606–613. [PubMed: 9510869]
28. Shvarev A, Bakker E. J Am Chem Soc 2003;125:11192–11193. [PubMed: 16220929]
29. Blomberg E, Claesson PM, Froeberg JC, Tilton RD. Langmuir 1994;10:2325–2334.
30. Pejcic B, De Marco R. Electrochim Acta 2006;51:6217–6229.
31. Toth K, Graf E, Horvai G, Pungor E, Buck RP. Anal Chem 1986;58:2741–2744.
32. Gemene KL, Shvarev A, Bakker E. Anal Chim Acta 2007;583:190–196. [PubMed: 17386545]

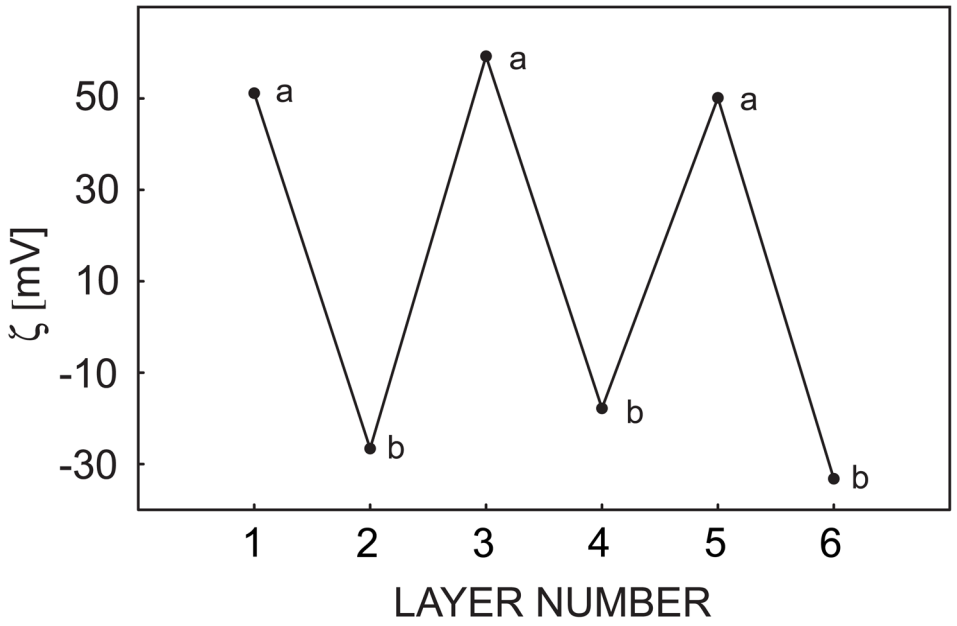

Fig. 1.
Zeta potential measurements of sensing material doped silanized silica micro-particles coated with alternate PEI and Alb multilayers as indicated.

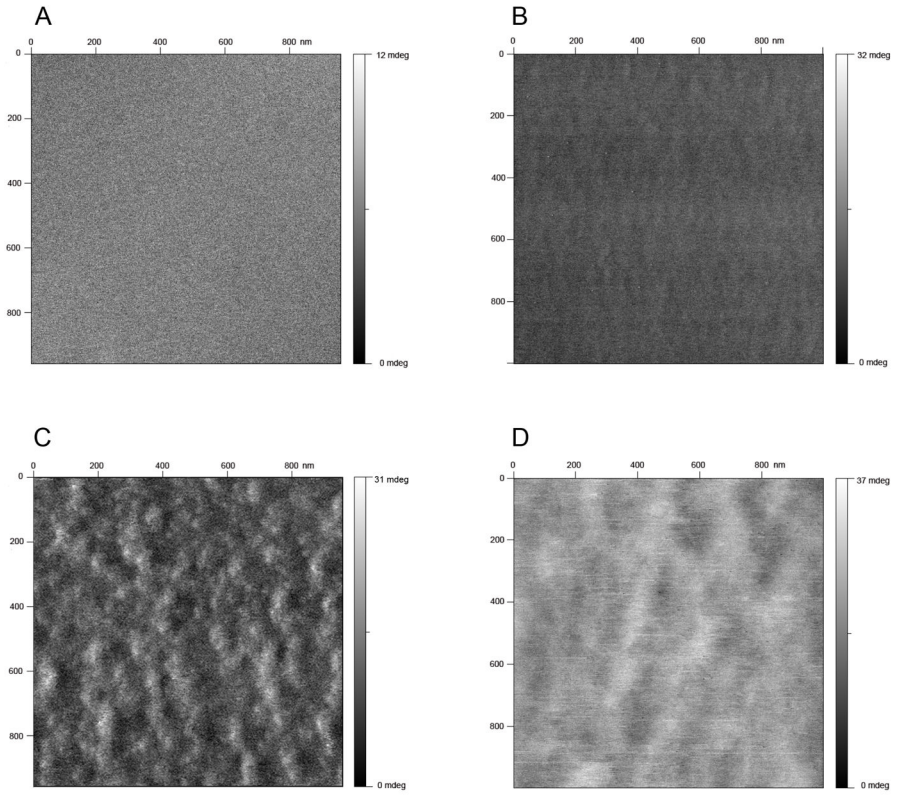

Fig. 2.

Tapping mode AFM phase images of multilayer deposited calcium-selective membrane on mica surface, (A) bare membrane surface (B) membrane coated with one layer PEI (C) membrane coated with PEI/Albumin double layers (D) membrane coated with PEI/Albumin/PEI triple layers.

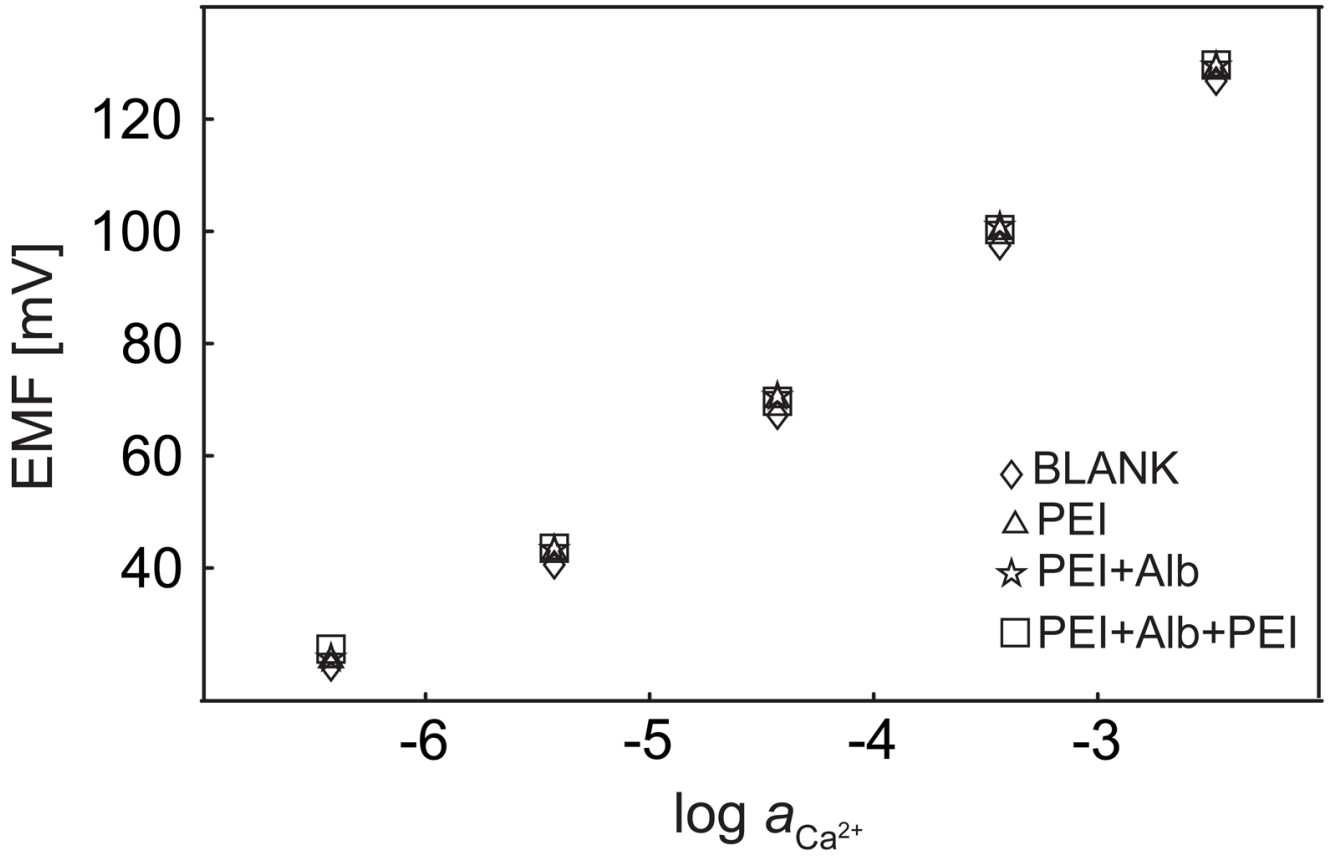

Fig. 3.
Zero-current potentiometry measurements of calcium-selective electrodes with polyelectrolyte multilayers covered on top of the sample side of the membrane, as indicated.

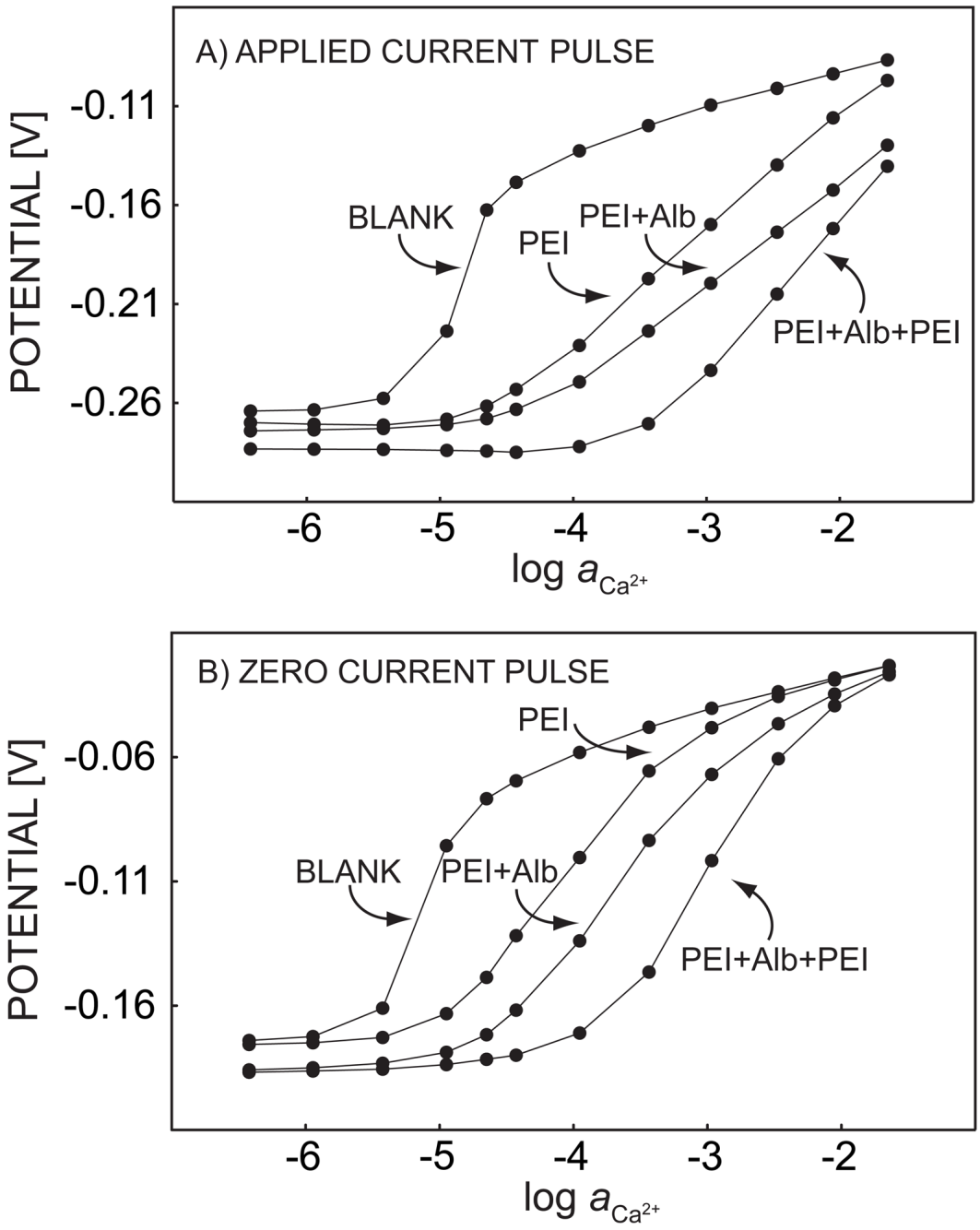

Fig. 4.

Pulstrode response of a calcium-selective membrane, sampled at the end of (A) a 1-s 0.5 μA/cm^2 cathodic current pulse and (B) a 0.5-s zero current pulse imposed immediately after the cathodic current pulse. The membrane is coated with PEI/Alb multilayers, as indicated.

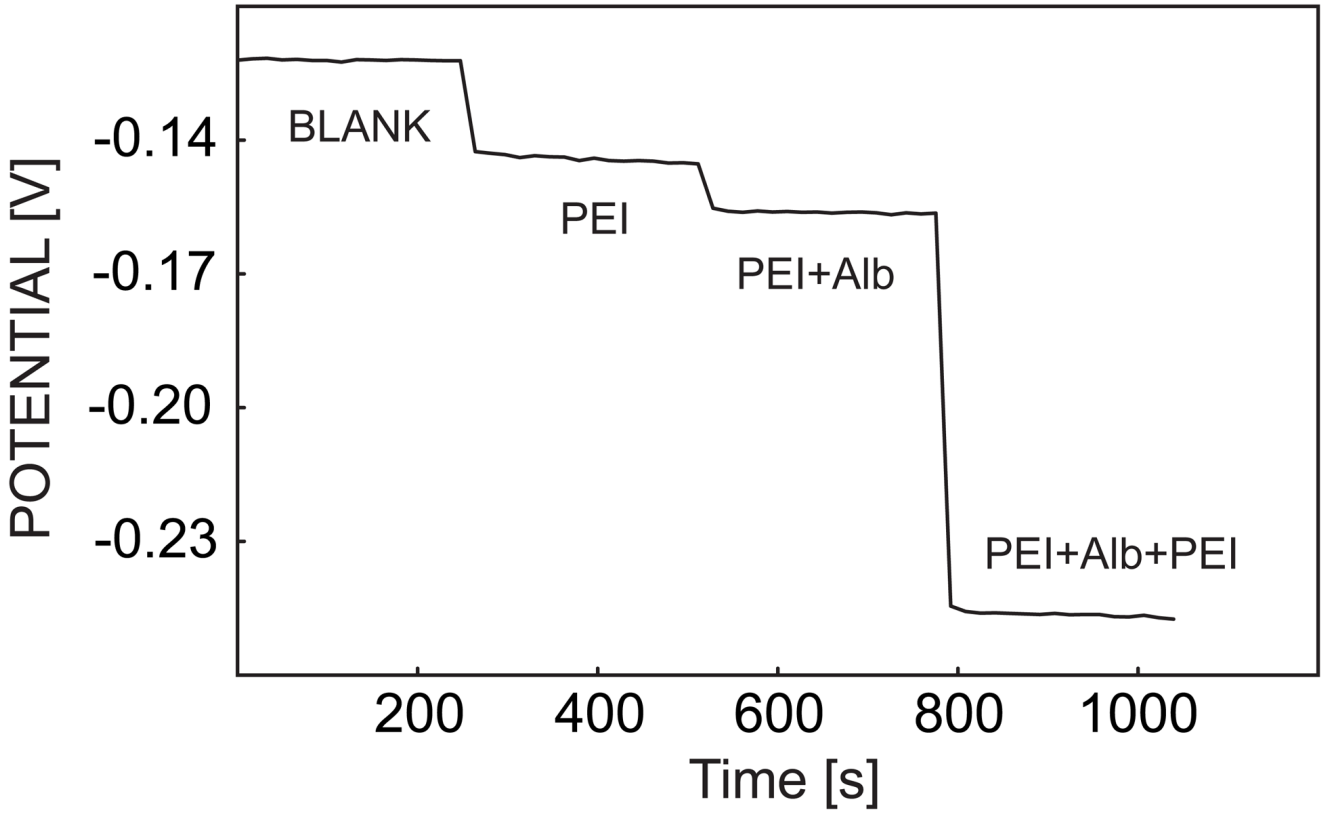

Fig. 5.
Time trace of pulstrode response of a calcium-selective membrane coated with indicated polyelectrolyte multilayers, sampled at the end of a 1-s 0.5 μA/cm^2 cathodic current pulse.

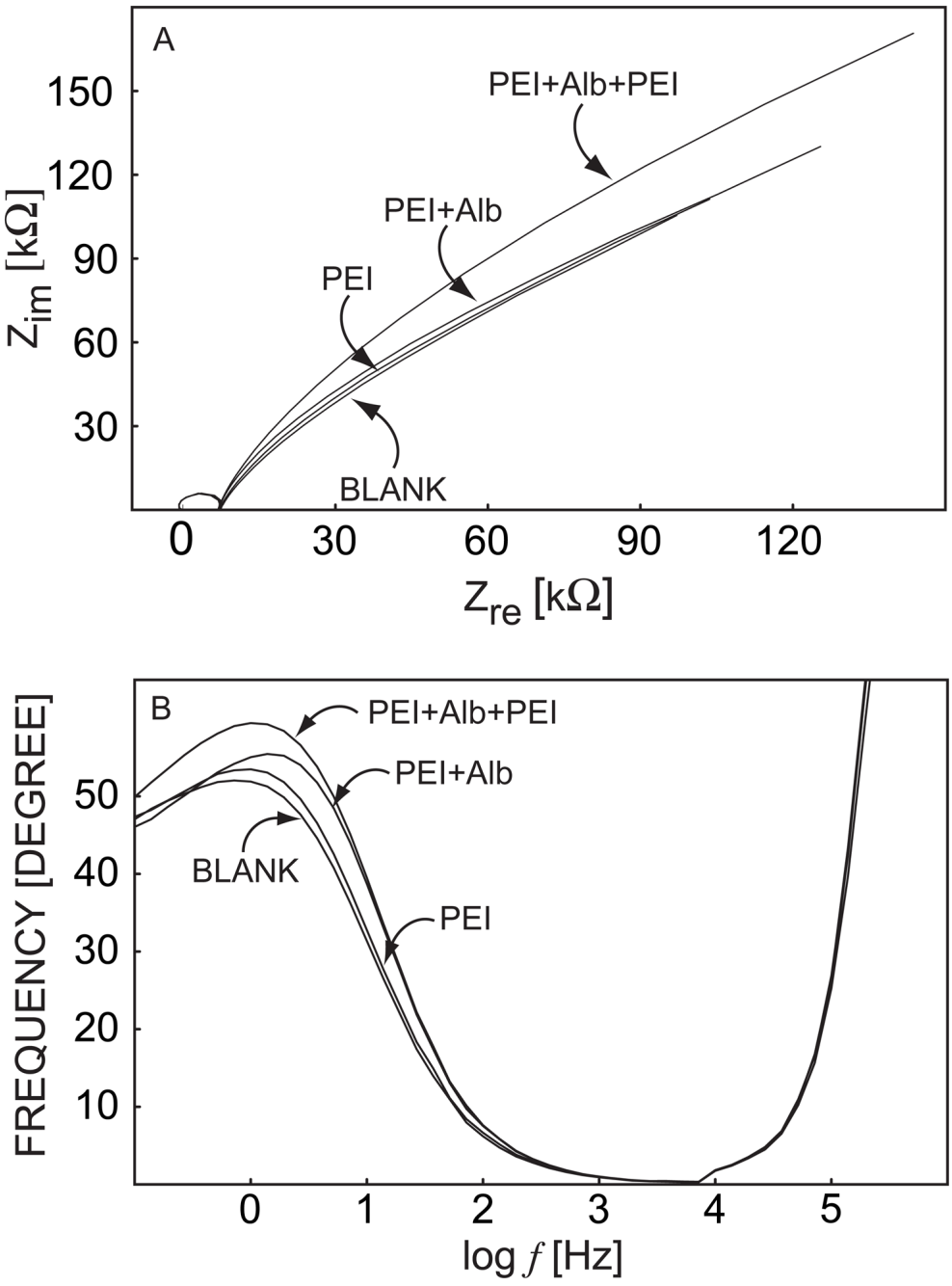

Fig. 6.
Electrochemical impedance spectra (Nyquist and Bode plots) for a calcium-selective membrane coated with PEI/Alb multilayers as indicated.

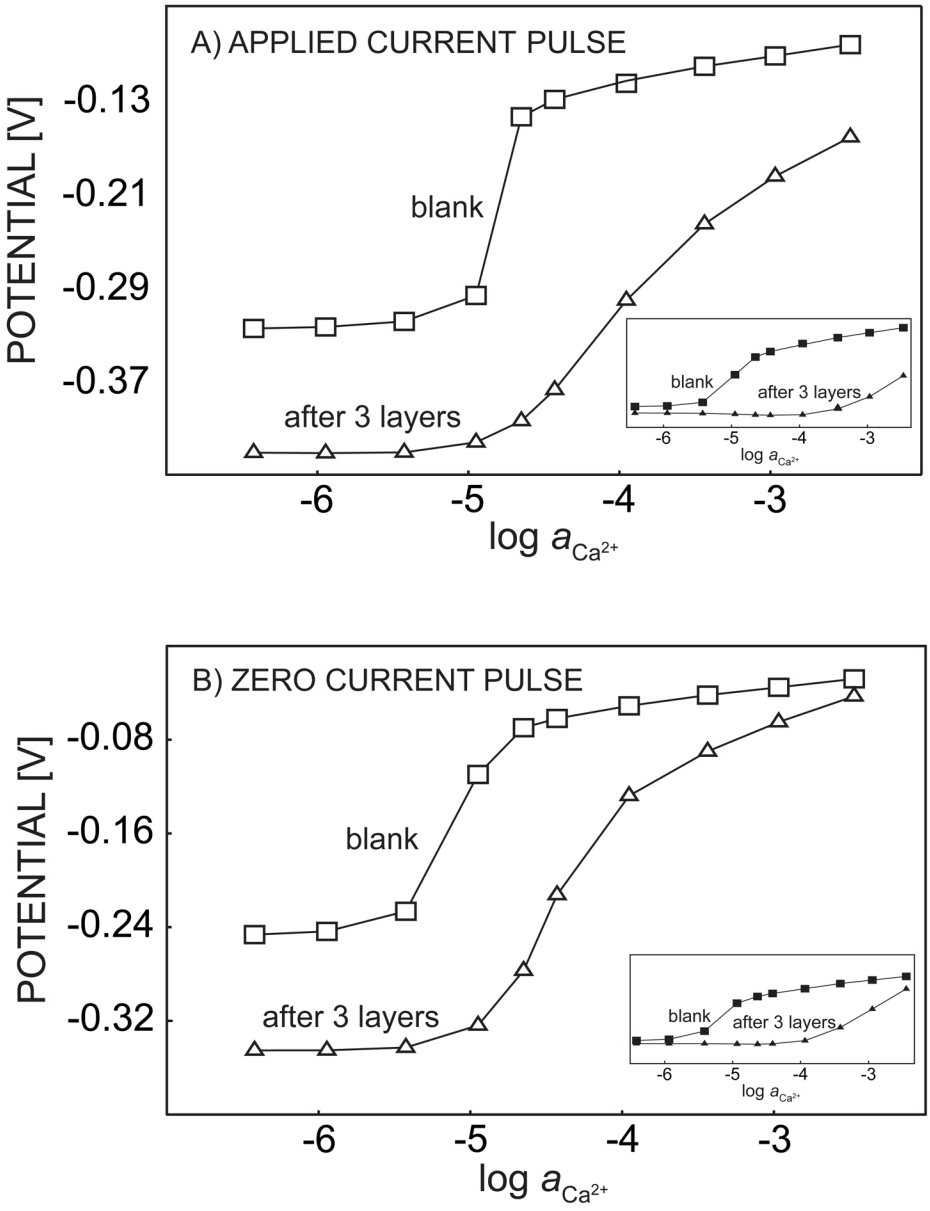

Fig. 7.

Pulstrode response of a calcium-selective membrane measured before and after the membrane is coated with PEI/Alb/PEI multilayers with a background electrolyte of 25 mM $MgSO_4$ or 0.1 M NaCl (inset) sampled at the end of (A) a 1-s 0.5 μA/cm^2 cathodic current pulse and (B) a 0.5-s zero current pulse imposed immediately after the cathodic current pulse.

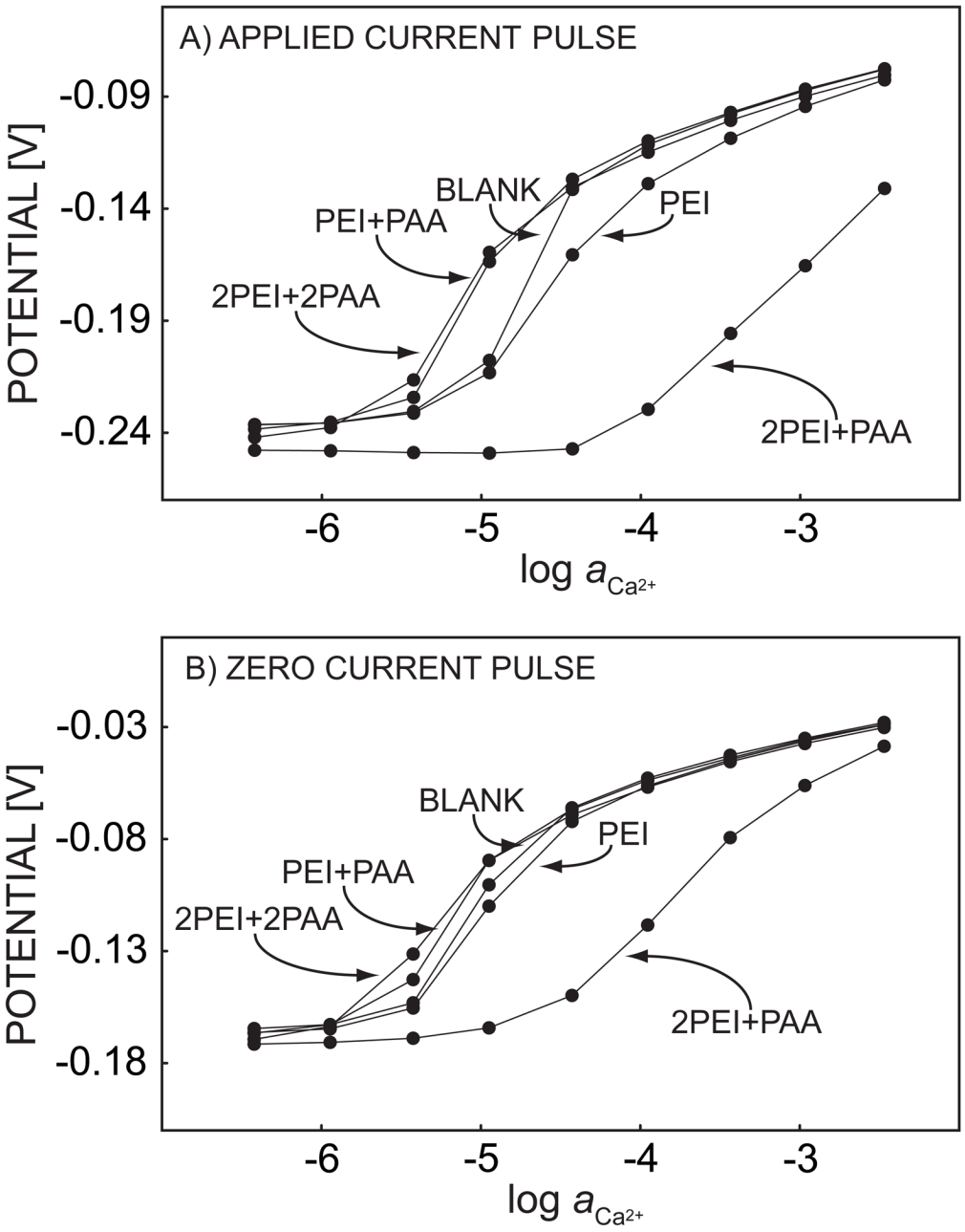

Fig. 8.

Pulstrode response of a calcium-selective membrane, sampled at the end of (A) a 1-s 0.5 μA/cm^2 cathodic current pulse and (B) a 0.5-s zero current pulse imposed immediately after the cathodic current pulse. The membrane is coated with PEI/PAA multilayers, as indicated.